Bioorganic & Medicinal Chemistry 19 (2011) 2298–2305

Contents lists available at ScienceDirect

Bioorganic & Medicinal Chemistry

journal homepage: www.elsevier.com/locate/bmc

Synthesis, biological evaluation and molecular modeling of novel triazole-containing berberine derivatives as acetylcholinesterase and β-amyloid aggregation inhibitors

Anding Shi, Ling Huang, Chuanjun Lu, Feng He *, Xingshu Li *

Institute of Drug Synthesis and Pharmaceutical Processing, School of Pharmaceutical Sciences, Sun Yat-sen University, Guangzhou 510006, China

ARTICLE INFO

Article history:
Received 2 December 2010
Revised 14 February 2011
Accepted 15 February 2011
Available online 18 February 2011

Keywords:
Acetylcholinesterase inhibitor
β-Amyloid aggregation inhibitors
Click chemistry
Berberine derivatives
Triazole-containing compounds

ABSTRACT

A series of novel triazole-containing berberine derivatives were synthesized via the azide–alkyne cycloaddition reaction. Their biological activity as inhibitors of both acetylcholinesterase (AChE) and butyrylcholinesterase (BuChE) were evaluated. Among them, compound **16d**, which featured a diisopropylamino substitution at the 4-position of triazole ring, was found to be a potent inhibitor of AChE, with IC_{50} value of 0.044 μM. Compound **18d**, which beares a butyl at the 4-position of the triazole ring, showed the highest potency of β-amyloid aggregation inhibition (77.9% at 20 μM). Molecular modeling studies indicated that the triazole moiety of berberine derivatives displayed a face-to-face π–π stacking interaction in a 'sandwich' form with the Trp84 (4.09 Å) and Phe330 (4.33 Å) in catalytic sites of AChE.

1. Introduction

Click chemistry, which provides near-perfect properties of green chemistry including simple and benign procedures, high yields, few byproducts and mild reaction conditions, has found applications in many research fields.[1,2] In pharmaceutical chemistry, with the choice of appropriate building blocks, it has been used for synthesis of the peroxisome proliferator-activated receptor γ (PPAR-γ) agonists for the treatment of type II diabetes,[3] multivalent triazole-linked neoglycoconjugates 1,3-dipolar cycloadditions,[4,5] preparation of an enzyme-bound inhibitor with acetylcholinesterase as a reaction vessel,[6] identification of HIV-1-PR inhibitors,[7] synthesis of drugs with anti-HIV activity and antimicrobial activity against Gram-positive bacteria,[8,9] the synthesis of a divalent single-chain fragment (di-scFv) of a monoclonal antibody (mAb),[10] and so on. Among them, the application of the azide–alkyne cycloaddition (AAC) reaction to acetylcholinesterase inhibitors (AChEIs) screening,[11,12] reported by Sharpless et al. made significant contributions to this field. The X-ray crystallographic studies of complexes of chosen AChEIs and mouse acetylcholinesterase (AChE)[11] suggested that the newly AAC-formed triazole moiety was employed as a valuable pharmacophore for its van der waals contract with the Phe-297 and Tyr-341 side chains. Therefore, from both fundamental and practical standpoints, it is still desirable to design, synthesize and evaluate new triazole-containing compounds for pharmacodynamic and pharmacological studies.

In recent years, numerous studies have indicated that besides cholinergic hypothesis, AChE is also involved with the etiology of Alzheimer's disease (AD) through PAS-induced β-amyloid (Aβ) aggregation, which is an early event in the neurodegenerative cascade of AD.[13] In consideration of these effects, different kinds of dual binding site AChEIs have been reported to possess inhibitory activities of both AChE and AChE-induced Aβ aggregation.[14–16] Usually, these AChEIs are made up of two pharmacophores linked by a appropriate chain, so that they can simultaneously bind to both the peripheral and catalytic sites (CAS) of AChE, which are separated by about 14 Å, located at the mouth and the bottom of the gorge of AChE, respectively. In our previous work, we designed and synthesized a series of novel molecules using berberine as the lead structure and found that they were capable of binding both the CAS and PAS of AChE.[17] Following this study, several series of novel berberine derivatives have been constructed and evaluated as potential dual binding site AChEIs. This paper discloses our work of designing, synthesizing, and evaluating a new series of triazole-containing berberine derivatives as multi-valent AchEIs and Aβ aggregation inhibitors.

2. Results and discussion

2.1. Design and synthesis of targeting compounds

Inspired from the excellent works of Sharpless, we designed a series of triazole-containing berberine derivatives and expected

* Corresponding authors. Tel./fax: +86 20 3994305 (X.L.).
E-mail address: lixsh@mail.sysu.edu.cn (X. Li).

0968-0896/$ - see front matter © 2011 Elsevier Ltd. All rights reserved.
doi:10.1016/j.bmc.2011.02.025

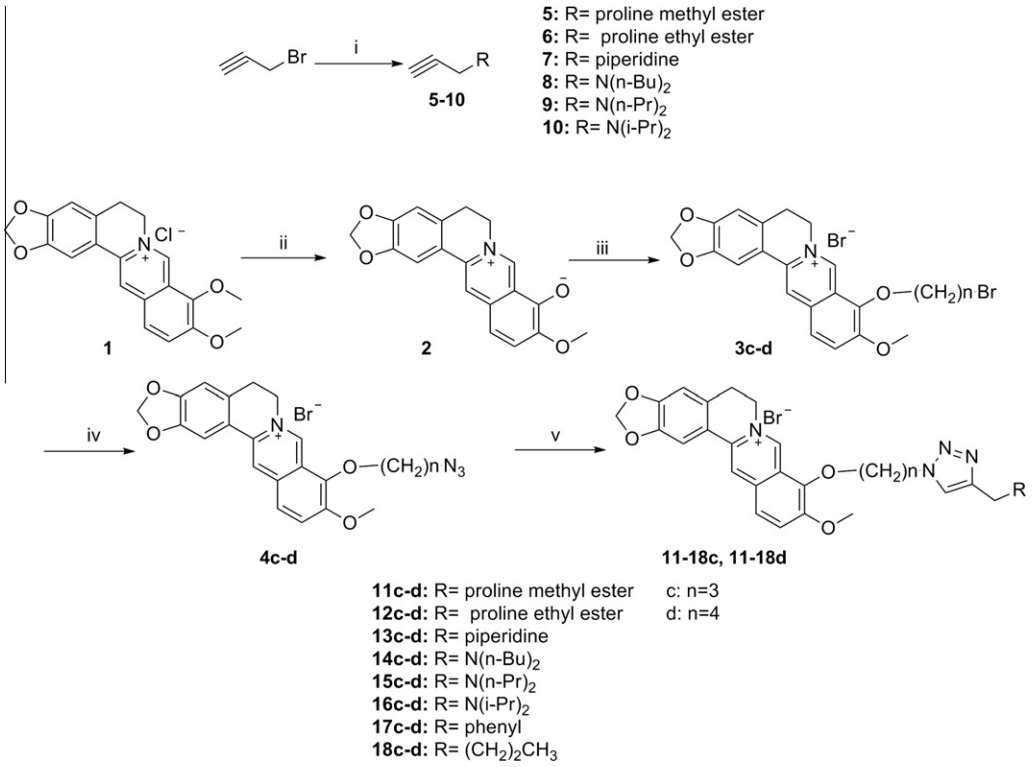

Scheme 1. 9-Substituted berberine derivatives **11**–**18c**, **11**–**18d**. Reagents and conditions:(i) RH, Cs_2CO_3, acetone; (ii) 190 °C, 20–30 mmHg, 15 min; (iii)Br(CH_2)*n*Br, DMF, 80 °C, 1–4 h; (iv) NaN_3, TBAI, DMF, 60 °C; (v) intermediates **5**–**10**, phenyl-allylene or 1-hexyne, $CuSO_4$, sodium ascorbate, DMF, 50 °C.

them to behave the follwing three discrete loci for effective inhibitory activity to AChE: (1) the berberine moiety binds to the PAS of AChE; (2) the triazole moeity binds to the intervening site; (3) the amino substituent at the 4-position of triazole ring binds to the CAS. The synthetic route of triazole-containing berberine derivatives is shown in Scheme 1. To begin with, berberrubine **2** was obtained in 66% yield through selective demethylation of berberine 1 at 190 °C under vacuum,[18] and then alkylated with 1,3-dibromopropane or 1,4-dibromobutane in DMF[19] to afford **3c** and **3d** in 66% and 75% yields, respectively. Compound **3c** or **3d** was equipped with an azide group by reacting with NaN_3 in the presence of tetrabutylammonium iodide (TBAI). On the other hand, intermediates **5**–**10** containing the propargyl substituted tertiary amine could be easily synthesized by displacement reaction of the corresponding secondary amine with propargyl bromide.[20] Finally, the generated azides **4c** or **4d** were reacted with the corresponding alkynes through Cu-catalyzed AAC to give the final products.

2.2. In vitro inhibition studies of AChE and BuChE

The AChE inhibitory effects of all triazole-containing berberine derivatives were examined by the method of Ellman et al.[21] on AChE from electric eel using commercial galanthamine as the reference standard. The IC_{50} values for AChE and BuChE inhibition are shown in Table 1. Most of the triazole-containing berberine derivatives were potent AChEIs with IC_{50} values ranging from micromolar to sub-micromolar. The optimal AChE inhibition potency (IC_{50} = 0.044 μM) was provided by compound **16d** featuring a diisopropylanmino substitution at the 4-position of the triazole ring. Mutation of this moiety from diisopropylanmino to straight-chain secondary amino (**14c**–**d, 15c**–**d**) or cyclic secondary amino substitutes (**13c**–**d**) lowered the inhibitory activity by an order of magnitude. This result implied that a flexible bulk of branch-chain secondary amines was favored toward the inhibitory activity. The inhibitory activity decreased even severer when the 4-substitution of triazole ring was replaced by a proline ester (**11c**–**d, 12c**–**d**). This loss of potency could be caused by both the relatively rigid five-membered ring and the ester group. Furthermore, the inhibition activity was also affected by the linkage between the triazole ring and berberine unit. Usually, a methylene tether length of three provided a better inhibitor than that of four, except for compounds **16c**–**d**, which revealed the highest inhibitory affinities. It is also worth noting that **17d**, with a phenyl group at the 4-position of the triazole ring, showed the most dramatic activity loss relative to its 3-methylene tethered homologue **17c** (1.32 μM vs 0.310 μM), suggesting that with the aromatic ring to occupy the CAS, a longer chain was not favorable. On the other hand, all these berberine triazole derivatives were uniformly more potent than berberine against butyrylcholinesterase (BuChE), which is consistent with the known theory that berberine primarily binds to the PAS of AChE, since there is no such domain within BuChE.

2.3. Kinetic study of AChE

To study the inhibitory mechanism for this class of AChEIs, one of the most potent inhibitors, compound **16d**, was chosen for further kinetic studies with AChE. The graphical presentation of steady-state inhibition data of compound **16d** for AchE is shown in Figure 1. The results revealed that there was an increasing slope and an increasing intercept at higher inhibitor concentrations, indicating a mixed type inhibitory behavior for compound **16d** with binding at both the CAS and PAS of AChE, which was similar with the model of berberine-derived AChEIs we previously reported.

2.4. Molecular modeling studies

To obtain useful information about the binding mode between triazole-containing berberine derivatives and AChE, a molecular

Table 1
In vitro inhibition IC_{50} (μM) and selectivity of compounds **1**, **11–18c**, **11–18d**, for AChE and BuChE

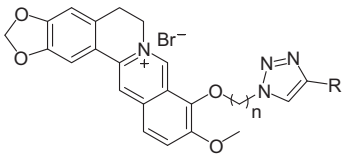

Compound	R	*n*	IC_{50} (μM)		Selectivity for AChE[c]
			AChE/ACh[a]	BuChE/BuCh[b]	
1	Berberine	—	0.374 ± 0.024	18.2 ± 0.683	48.6
11c	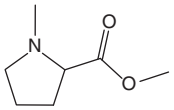	3	0.785 ± 0.023	5.30 ± 0.106	6.75
11d		4	0.903 ± 0.047	5.27 ± 0.378	5.84
12c	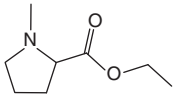	3	0.601 ± 0.147	2.40 ± 0.258	3.99
12d		4	0.606 ± 0.052	2.32 ± 0.304	3.83
13c	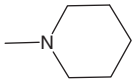	3	0.108 ± 0.001	4.24 ± 0.071	39.3
13d		4	0.274 ± 0.011	5.73 ± 0.09	20.9
14c	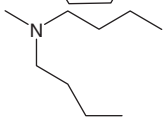	3	0.243 ± 0.006	2.06 ± 0.106	8.48
14d		4	0.469 ± 0.040	5.46 ± 0.106	11.6
17c	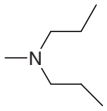	3	0.140 ± 0.011	1.58 ± 0.099	11.3
15d		4	0.270 ± 0.018	4.77 ± 0.148	17.7
16c	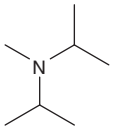	3	0.067 ± 0.003	2.86 ± 0.396	42.7
16d		4	0.044 ± 0.001	6.21 ± 0.127	141
17c		3	0.310 ± 0.029	2.21 ± 0.138	7.13
17d		4	1.32 ± 0.196	1.50 ± 0.131	1.14
18c		3	0.165 ± 0.015	4.06 ± 0.250	24.6
18d		4	0.201 ± 0.017	2.02 ± 0.500	10.0
Galanthamine	—	—	0.623 ± 0.099	15.7 ± 0.787	25.3

[a] 50% inhibitory concentration (means ± SEM of three experiments) of AChE from electric eel.
[b] 50% inhibitory concentration (means ± SEM of three experiments) of BuChE from equine serum.
[c] Selectivity for AChE = IC_{50} (BuChE)/IC_{50} (AChE).

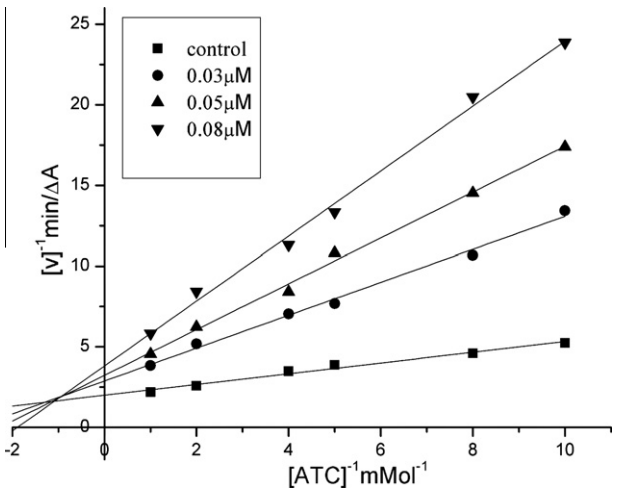

Figure 1. Steady state inhibition by **16d** of AChE hydrolysis of ATCh; the plots show mixed-type inhibition for **16d** on AchE.

docking simulation was performed based on a well-known complex between AChE from Torpedo californica (TcAChE) and bis(5)-tacrine (PDB code 2CMF). Triazole-containing compound **16d**, the most potent AChE inhibitor, was chosen to explore the ligand-protein interactions. The position of compound **16d** with respect to the key residues in the binding site is shown in Figure 2. Similar to the berberine derivatives we previously reported,[17] compound **16d** could simultaneously interact with the CAS and PAS of AChE. The berberine moiety of **16d** adopted an appropriate orientation that allows its B ring to form a π–π stacking with the indole ring Trp279 (4.29 Å) in PAS. A hydrogen bond between the 9-oxygen atom of the berberine moiety and the backbone OH group of Tyr121 (2.77 Å) existed, which was consistent with the results of our previous reports. However, the triazole moiety, which was designed to occupy the intervening site, was found to positioned at the CAS, displaying an unexpected face-to-face π–π stacking interaction in a 'sandwich' form with Trp84 (4.09 Å) and Phe330 (4.33 Å). While the diisopropylamino moiety formed hydrophobic interactions with Ser81, Ser122 and Try121, instead of occupying the CAS as predicted. This difference from the sharpless report might be due to the relatively long and narrow structure of berber-

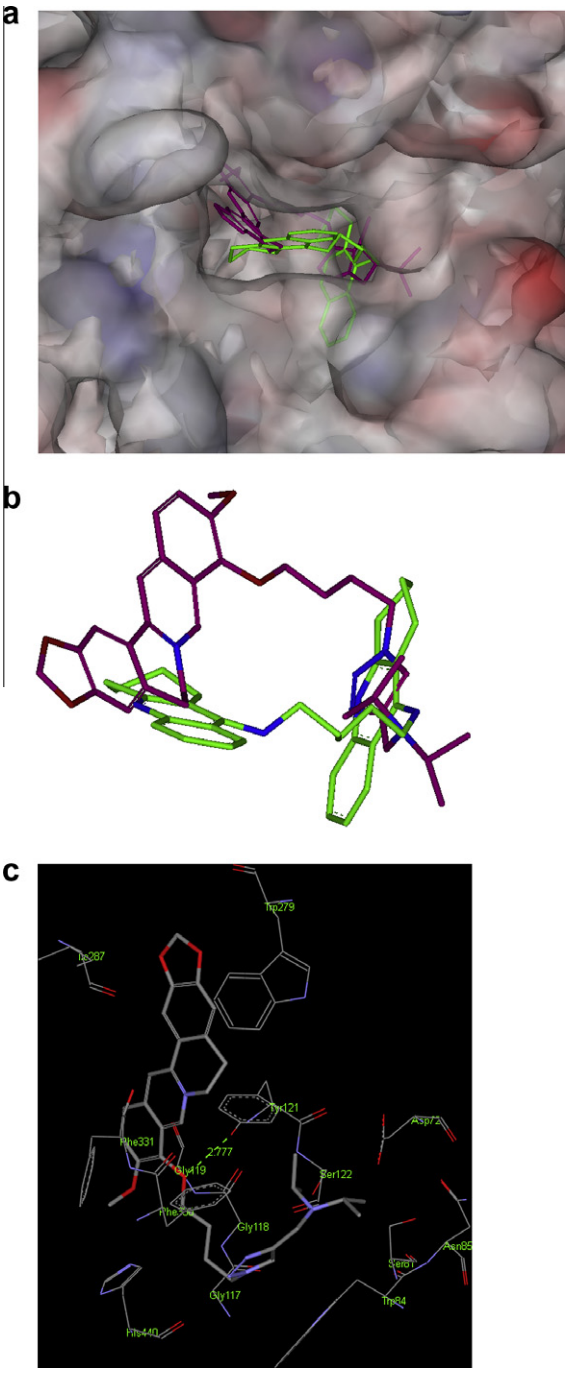

Figure 2. Docking models of the compound-enzyme complex. (a) Stereoviews looking down the gorge of TcAChE binding with **16d** (colored in purple) and the original ligand of the X-ray structure bis(5)-tacrine (colored green). (b) Superposition of modeled structure of compound **16d** (colored in purple) with X-ray crystal structure of TcAChE binding with bis(5)-tacrine (colored in green, PDB entry: 2CMF). (c) Representation of compound **16d** docked into the binding site of AChE highlighting the protein residues that form the main interactions with the inhibitor. Hydrogen-bonding interaction between ligand and residues Tyr121 is shown with the green line.

ine, which uses B ring to bind to the PAS, C and D rings stretch into the gorge. Thus, the triazloe moiety could reach the CAS of AChE.

2.5. Effects on the $A\beta_{1-42}$ peptide aggregation

The ability of several triazole-containing berberine derivatives to reduce $A\beta_{1-42}$ self-aggregation was studied through a thioflavin T-based fluorimetric assay with curcumin (Cur) as standard compound. The results are summarized in Figure 3. It is interesting that all berberine derivatives showed higher potencies compared to that of the curcumin (52.1%) and the parent compound, berberine (36.3%). Among them, compound **18d**, with a butyl at the 4-position of the triazole ring, showed the highest potency of Aβ aggregation inhibition (77.9%). On the other hand, compound **16d**, which was the most potent AChE inhibitor, gave 52.8% of the inhibition potency. Compound **14d**, with a *N*,*N*-dibutyl amino at the end of the 4-substitute of the triazole ring, gave 71.7% inhibition potency, while its homologous **15d**, with a *N*,*N*-dipropyl amino at the same possition, provided 62.5% of that. The results implied that straight chain structure with enough length at the end of the 4-substitute of the triazole ring would be favourable for $A\beta_{1-42}$ peptide aggregation inhibition. However, branched chain (**16d**, a *N*,*N*-di-isobutyl amino group, 52.8%), ring structures (**13d**, a cyclic secondary amino group, 63.7%, and **17d**, a phenyl group, 60.6%) at the end of the 4-substitute of the triazole ring were found less favourable.

3. Conclusion

In summary, this study revealed the construction of a new series of triazole-containing berberine derivatives using click chemistry and their evaluation as potential multi-valent inhibitors of AChE, BuChE and Aβ aggregation. Among the triazole-containing compounds tested, compound **16d**, featuring a diisopropylanmino substitute at the 4-position of the triazole ring, displayed the highest inhibitory activity with an IC_{50} value of 0.044 μM against AChE. Replacement of the diisopropylanmino substitution at 4-position of the triazole ring with straight-chain secondary amino, cyclic secondary amino or nonamino weakened the inhibition activity drastically. Meanwhile, compound **18d**, which beares a butyl at the 4-position of the triazole ring and showed good inhibitory activity against AChE (with an IC_{50} value of 0.201 μM), gave the highest potency of Aβ aggregation inhibition (77.9%). Molecular modeling simulations of the AChE inhibitor complex showed that the triazole moieties in berberine derivatives actually contributed to the inhibitory activities through interacting with the CAS of AChE. In addition, kinetic studies indicated that these compounds exhibited a mixed type inhibition for both the catalytic active site and the peripheral anionic site. Further investigations of these compounds as AD candidates are in progress.

4. Experimental section

4.1. Chemistry

The ^1H NMR spectra were recorded with TMS as the internal standard on a Varian 400 MHz spectrometer. Coupling constants were given in Hz. MS spectra were recorded on a Agilent LC–MS 6120 instrument with an ESI mass selective detector. High-resolution mass spectra were obtained by Shimadazu LCMS-IT-TOF mass spectrometere. Flash column chromatography was performed with silica gel (200–300 mesh) purchased from Qingdao Haiyang Chemical Co. Ltd or alumina from Sinopharm Chemical Reagent Co. Ltd. All the reactions were monitored by thin layer chromatography on silica gel. Berberine chloride was isolated from Chinese herbal medicine *Cryptocarya* chinensis Franch and recrystallized from hot water. Compound **2** was prepared according to the reported procedure.[20] Intermediates **3c** and **3d** were also synthesized based on previous report.[21] Intermediates **5–10** were synthesized as the following procedures.

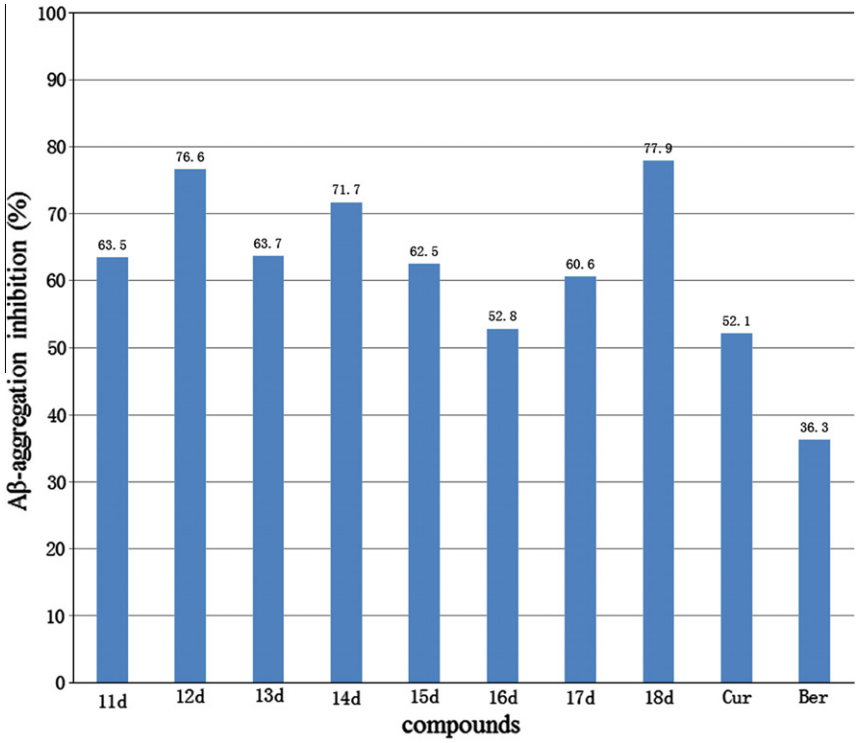

Figure 3. Effects on the $A\beta_{1-42}$ peptide aggregation inhibition at 20 μM of some triazole-containing berberine derivatives.

4.2. General procedures for the preparation of 5–10

Propargyl bromide (0.5 mmol) was dropwise added to a mixture of Cs_2CO_3 (0.5 mmol), acetone (30 mL) and the corresponding secondary amine (0.5 mmol) at 0 °C. The mixture was stirred overnight at room temperature and then filtered. The filtrates was evaporated to dryness to afford the target productes as an orange-brown oil. which was directly used for the next step without purification.

4.3. General procedures for the preparation of 4c–d

To a solution of compounds **3c** or **3d** (2 mmol) in DMF (15 mL), NaN_3 (20 mmol) and TBAI (12 mmol) were added at the room temperature. After stirred at 60 °C for 6 h, the mixture was cooled to room temperature, filtered, washed with water and dried under vaccum, giving the desired product as bright yellow solid.

4.3.1. 9-*O*-(3-Azido-propyl) berberine bromide (4c)

Intermediate **3c** was treated with NaN_3 and TBAI according to general procedure to give the target product **4c** as bright yellow solid. Yield 75%. ^{1}H NMR (400 MHz,) δ 9.78 (s, 1H), 8.93 (s, 1H), 8.20 (d, J = 9.2 Hz, 1H), 8.00 (d, J = 9.1 Hz, 1H), 7.79 (s, 1H), 7.09 (s, 1H), 6.17 (s, 2H), 4.94 (t, J = 6.0 Hz, 2H), 4.36 (t, J = 6.2 Hz, 2H), 4.06 (s, 3H), 3.66 (t, J = 6.7 Hz, 2H), 3.26–3.16 (m, 2H), 2.14 (p, J = 6.5 Hz, 2H). LC/MS (ESI) m/z: [M−Br]+ 405.4.

4.3.2. 9-*O*-(3-Azido-butyl) berberine bromide (4d)

Intermediate **3d** was treated with NaN_3 and TBAI according to general procedure to give the target product **4d** as bright yellow solid. Yield 72%; ^{1}H 1H NMR (400 MHz,) δ 9.77 (s, 1H), 8.94 (s, 1H), 8.20 (d, J = 9.0 Hz, 1H), 7.99 (d, J = 9.0 Hz, 1H), 7.80 (s, 1H), 7.09 (s, 1H), 6.18 (s, 2H), 4.95 (t, J = 5.8 Hz, 2H), 4.31 (t, J = 6.1 Hz, 2H), 4.06 (s, 3H), 3.47 (t, J = 6.6 Hz, 2H), 3.21 (t, J = 5.7 Hz, 2H), 1.99–1.89 (m, 2H), 1.85–1.75 (m, 2H); LC/MS (ESI) m/z: $[M-Br]^+$ 419.3.

4.4. General procedures for the preparation of 11–18c, 11–18d

$CuSO_4$ (0.32 mmol), sodium ascorbate (1.3 mmol) and compound **4c** or **4d** (0.65 mmol) were stirred in DMF, corresponding terminal alkyne (dissoluted in DMF) was dropwise added as the temperature rising to 50°C. The mixture was stirred at 50°C for 5 h, and then evaporated under vaccum, the crude product was chromatographed on an Al_2O_3 column, eluted with $CHCl_3$/MeOH (100:1–50:1) to afford the final product.

4.4.1. 9-*O*-{3-{4-[(2-Methoxycarbonyl-pyrrolidin-1-yl)methyl]-1*H*-1,2,3-triazol-1-yl}propyl}berberine bromide (11c)

Intermediate **4c** was treated with $CuSO_4$, sodium ascorbate and methyl 1-(prop-2-ynyl)pyrrolidine-2-carboxylate (**5**) according to general procedure to give the target product **11c** as yellow semi-solid. Yield 38.1%; $[\alpha]_D^{20} = -12.9$ (0.1, $CHCl_3$); ^{1}H 1H NMR (400 MHz,) δ 9.84 (s, 1H), 8.95 (s, 1H), 8.19 (d, J = 9.0 Hz, 1H), 8.07 (s, 1H), 8.00 (d, J = 8.9 Hz, 1H), 7.80 (s, 1H), 7.10 (s, 1H), 6.18 (s, 2H), 4.98 (t, J = 5.7 Hz, 2H), 4.67 (t, J = 6.3 Hz, 2H), 4.26 (t, J = 5.8 Hz, 2H), 4.03 (s, 3H), 3.88 (d, J = 13.9 Hz, 1H), 3.70 (d, J = 13.9 Hz, 1H), 3.57 (s, 3H), 3.23–3.20 (m, 2H), 2.92–2.85 (m, 1H), 2.43–2.32 (m, 2H), 2.04–1.86 (m, 3H), 1.81–1.72 (m, 1H), 1.70–1.62 (m, 2H); LC/MS (ESI) m/z: $[M-Br]^+$ 572.3; HRMS m/z $[M-Br]^+$ Calcd for $C_{31}H_{33}N_5O_6$ 572.2509, Found 572.2522.

4.4.2. 9-*O*-{3-{4-[(2-Methoxycarbonyl-pyrrolidin-1-yl)methyl]-1*H*-1,2,3-triazol-1-yl}butyl}berberine bromide (11d)

Intermediate **4d** was treated with $CuSO_4$, sodium ascorbate and methyl 1-(prop-2-ynyl)pyrrolidine-2-carboxylate (**5**) according to general procedure to give the target product **11d** as yellow solid. Yield 33.8%; mp 172.4–173.1; $[\alpha]_D^{20} = -12.5$ (0.4, $CHCl_3$); ^{1}H NMR (400 MHz,) δ 9.75 (s, 1H), 8.93 (s, 1H), 8.19 (d, J = 9.0 Hz, 1H),

7.99 (d, J = 9.3 Hz, 2H), 7.80 (s, 1H), 7.10 (s, 1H), 6.17 (s, 2H), 4.95 (t, 5.6Hz, 2H), 4.45 (t, J = 6.6 Hz, 2H), 4.28 (t, J = 5.9 Hz, 2H), 4.04 (s, 3H), 3.85 (d, J = 13.8 Hz, 1H), 3.69 (d, J = 13.9 Hz, 1H), 3.58 (s, 3H), 3.22 (t, J = 6.6 Hz 2H), 2.92–2.82 (m, 1H), 2.42–2.36 (m, 2H), 2.12–2.04 (m, 2H), 2.00–1.92 (m, 1H), 1.85–1.72 (m, 3H), 1.72–1.62 (m, 2H); LC/MS (ESI) m/z: $[M-Br]^+$ 586.3; HRMS m/z $[M-Br]^+$ Calcd for $C_{32}H_{35}N_5O_6$ 586.2666, Found 586.2643.

4.4.3. 9-*O*-{3-{4-[(2-Ethoxycarbonyl-pyrrolidin-1-yl)methyl]-1*H*-1,2,3-triazol-1-yl}propyl}berberine bromide (12c)

Intermediate **4c** was treated with $CuSO_4$, sodium ascorbate and ethyl 1-(prop-2-ynyl)pyrrolidine-2-carboxylate (**6**) according to general procedure to give the target product **12c** as yellow semisolid. Yield 42.3%; $[\alpha]_D^{20} = -13.5$ (0.2, $CHCl_3$); ^{1}H NMR (400 MHz,) δ 9.84 (s, 1H), 8.94 (s, 1H), 8.19 (d, J = 9.2 Hz, 1H), 8.06 (s, 1H), 8.00 (d, J = 9.1 Hz, 1H), 7.80 (s, 1H), 7.10 (s, 1H), 6.18 (s, 2H), 4.98 (t, J = 5.8Hz, 2H), 4.67 (t, J = 6.8 Hz, 2H), 4.26 (t, J = 5.9 Hz, 2H), 4.08–3.97 (m, 5H), 3.88 (d, J = 13.9 Hz, 1H), 3.70 (d, J = 13.8 Hz, 1H), 3.23 (t, J = 6.8 Hz, 4H), 2.91–2.84 (m, 1H), 2.45–2.41 (m, 2H), 2.03–1.88 (m, 1H), 1.81–1.72 (m, 1H), 1.72–1.59 (m, 2H), 1.15 (t, J = 7.1 Hz, 3H); LC/MS (ESI) m/z: $[M-Br]^+$ 586.3; HRMS m/z $[M-Br]^+$ Calcd for $C_{32}H_{35}N_5O_6$ 586.2666, Found 586.2637.

4.4.4. 9-*O*-{3-{4-[(2-Ethoxycarbonyl-pyrrolidin-1-yl)methyl]-1*H*-1,2,3-triazol-1-yl}butyl}berberine bromide (12d)

Intermediate **4d** was treated with $CuSO_4$, sodium ascorbate and ethyl 1-(prop-2-ynyl)pyrrolidine-2-carboxylate (**6**) according to general procedure to give the target product **12d** as yellow semisolid. Yield 37.1%; $[\alpha]_D^{20} = -14.0$ (0.1, $CHCl_3$); ^{1}H NMR (400 MHz,) δ 9.76 (s, 1H), 8.94 (s, 1H), 8.19 (d, J = 9.2 Hz, 1H), 7.99 (d, J = 10.1 Hz, 2H), 7.80 (s, 1H), 7.10 (s, 1H), 6.17 (s, 2H), 4.96 (t, J = 6.4Hz, 2H), 4.46 (t, J = 6.8 Hz, 2H), 4.29 (t, J = 6.2 Hz, 2H), 4.08–4.01 (m, 5H), 3.86 (d, J = 13.8 Hz, 1H), 3.69 (d, J = 13.8 Hz, 1H), 3.22 (t, J = 6.8Hz, 2H), 2.92–2.83 (m, 1H), 2.45–2.37 (m, 2H), 2.14–2.04 (m, 2H), 2.02–1.93 (m, 1H), 1.86–1.74 (m, 3H), 1.71–1.62 (m, 2H), 1.16 (t, J = 7.1 Hz, 3H); LC/MS (ESI) m/z: $[M-Br]^+$ 600.3; HRMS m/z $[M-Br]^+$ Calcd for $C_{33}H_{37}N_5O_6$ 600.2822, Found 600.2818.

4.4.5. 9-*O*-{3-{4-[(Piperidin-1-yl)methyl]-1*H*-1,2,3-triazol-1-yl}propyl}berberine bromide (13c)

Intermediate **4c** was treated with $CuSO_4$, sodium ascorbate and 1-(prop-2-ynyl)piperidine (**7**) according to general procedure to give the target product **13c** as yellow solid. Yield 30.7%; mp 140.5–143.6; ^{1}H NMR (400 MHz,) δ 9.84 (s, 1H), 8.95 (s, 1H), 8.20 (d, J = 9.2 Hz, 1H), 8.09 (s, 1H), 8.01 (d, J = 9.2 Hz, 1H), 7.80 (s, 1H), 7.10 (s, 1H), 6.18 (s, 2H), 4.99 (t, J = 6.0 Hz, 2H), 4.68 (t, J = 6.9 Hz, 2H), 4.28 (t, J = 6.0 Hz, 2H), 4.03 (s, 3H), 3.54 (s, 2H), 3.23 (t, J = 6.8 Hz, 2H), 2.47–2.41 (m, 2H), 2.38–2.31 (m, 4H), 1.50–1.41 (m, 4H), 1.38–1.29 (m, 2H); LC/MS (ESI) m/z: $[M-Br]^+$ 528.2; HRMS m/z $[M-Br]^+$ Calcd for $C_{30}H_{33}N_5O_4$ 528.2611, Found 528.2598.

4.4.6. 9-*O*-{3-{4-[(Piperidin-1-yl)methyl]-1*H*-1,2,3-triazol-1-yl}butyl}berberine bromide (13d)

Intermediate **4d** was treated with $CuSO_4$, sodium ascorbate and 1-(prop-2-ynyl)piperidine (**7**) according to general procedure to give the target product **13d** as yellow solid. Yield 33.0%; mp 191.7–192.5; ^{1}H NMR (400 MHz,) δ 9.75 (s, 1H), 8.94 (s, 1H), 8.19 (d, J = 9.2 Hz, 1H), 8.05–7.96 (m, 2H), 7.80 (s, 1H), 7.10 (s, 1H), 6.18 (s, 2H), 4.95 (t, J = 6.0 Hz, 2H), 4.46 (t, J = 6.9 Hz, 2H), 4.29 (t, J = 6.3 Hz, 2H), 4.05 (s, 3H), 3.54 (s, 2H), 3.22 (t, J = 6.8 Hz, 2H), 2.46–2.24 (m, 4H), 2.15–2.05 (m, 2H), 1.88–1.78 (m, 2H), 1.52–1.41 (m, 4H), 1.40–1.30 (m, 2H); LC/MS (ESI) m/z: $[M-Br]^+$ 542.3; HRMS m/z $[M-Br]^+$ Calcd for $C_{31}H_{35}N_5O_4$ 542.2767, Found 542.2750.

4.4.7. 9-*O*-{3-{4-[(*N*,*N*-Dibutyl-amino)methyl]-1*H*-1,2,3-triazol-1-yl}propyl}berberine bromide (14c)

Intermediate **4c** was treated with $CuSO_4$, sodium ascorbate and *N*-butyl-*N*-(prop-2-ynyl)butan-1-amine (**8**) according to general procedure to give the target product **14c** as yellow semisolid. Yield 34.2%; ^{1}H NMR (400 MHz,) δ 9.85 (s, 1H), 8.95 (s, 1H), 8.20 (d, J = 9.0 Hz, 1H), 8.01 (t, J = 9.9 Hz, 2H), 7.80 (s, 1H), 7.10 (s, 1H), 6.18 (s, 2H), 4.98 (t, J = 5.2 Hz, 2H), 4.68 (t, J = 6.4 Hz, 2H), 4.26 (t, J = 5.5 Hz, 2H), 4.03 (s, 3H), 3.64 (s, 2H), 3.24 (t, J = 6.3 Hz, 2H), 2.45–2.41 (m, 2H), 2.31 (m, 4H), 1.38 (m, 4H), 1.22 (m, 4H), 0.81 (t, J = 7.2 Hz, 6H); LC/MS (ESI) m/z: $[M-Br]^+$ 572.3; HRMS m/z $[M-Br]^+$ Calcd for $C_{33}H_{41}N_5O_4$ 572.3237, Found 572.3221.

4.4.8. 9-*O*-{3-{4-[(*N*,*N*-Dibutyl-amino)methyl]-1*H*-1,2,3-triazol-1-yl}butyl}berberine bromide (14d)

Intermediate **4d** was treated with $CuSO_4$, sodium ascorbate and *N*-butyl-*N*-(prop-2-ynyl)butan-1-amine (**8**) according to general procedure to give the target product **14d** as yellow semisolid. Yield 30.7%; mp 190.5–191.6; ^{1}H NMR (400 MHz,) δ 9.74 (s, 1H), 8.93 (s, 1H), 8.19 (d, J = 9.2 Hz, 1H), 8.01–7.94 (m, 2H), 7.80 (s, 1H), 7.10 (s, 1H), 6.17 (s, 2H), 4.96 (t, J = 6.1 Hz, 2H), 4.46 (t, J = 6.8 Hz, 2H), 4.28 (t, J = 6.3 Hz, 2H), 4.04 (s, 3H), 3.60 (s, 2H), 3.22 (t, J = 6.6 Hz, 2H), 2.27 (t, J = 7.0 Hz, 4H), 2.14–2.04 (m, 2H), 1.84–1.76 (m, 2H), 1.42–1.31 (m, 4H), 1.26–1.16 (m, 4H), 0.82 (t, J = 7.3 Hz, 6H); LC/MS (ESI) m/z: $[M-Br]^+$ 586.3; HRMS m/z $[M-Br]^+$ Calcd for $C_{34}H_{43}N_5O_4$ 586.3393, Found 586.3384.

4.4.9. 9-*O*-{3-{4-[(*N*,*N*-Dipropyl-amino)methyl]1*H*-1,2,3-triazol-1-yl}propyl}berberine bromide (15c)

Intermediate **4c** was treated with $CuSO_4$, sodium ascorbate and *N*,*N*-dipropylprop-2-yn-1-amine (**9**) according to general procedure to give the target product **15c** as yellow semisolid. Yield 39.3%; ^{1}H NMR (400 MHz,) δ 9.83 (s, 1H), 8.94 (s, 1H), 8.19 (d, J = 9.2 Hz, 1H), 8.01 (t, J = J = 8.9 Hz, 2H), 7.80 (s, 1H), 7.10 (s, 1H), 6.18 (s, 2H), 4.97 (t, 5.9 Hz, 2H), 4.68 (t, J = 6.7 Hz, 2H), 4.26 (t, J = 5.8 Hz, 2H), 4.03 (s, 3H), 3.65 (s, 2H), 3.23 (t, J = 6.7 Hz, 2H), 2.46–2.38 (m, 2H), 2.32–2.23 (m, 4H), 1.41 (m, 4H), 0.79 (t, J = 7.2 Hz, 6H); LC/MS (ESI) m/z: $[M-Br]^+$ 544.3; HRMS m/z $[M-Br]^+$ Calcd for $C_{31}H_{37}N_5O_4$ 544.2924, Found 544.2937.

4.4.10. 9-*O*-{3-{4-[(*N*,*N*-Dipropyl-amino)methyl]-1*H*-1,2,3-triazol-1-yl}butyl}berberine bromide (15d)

Intermediate **4d** was treated with $CuSO_4$, sodium ascorbate and *N*,*N*-dipropylprop-2-yn-1-amine (**9**) according to general procedure to give the target product **15d** as yellow solid. Yield 38.0%; mp 169.6–170.5; ^{1}H NMR (400 MHz,) δ 9.75 (s, 1H), 8.94 (s, 1H), 8.19 (d, J = 9.2 Hz, 1H), 7.99 (d, J = 9.1 Hz, 2H), 7.80 (s, 1H), 7.10 (s, 1H), 6.18 (s, 2H), 4.95 (t, J = 6.2 Hz, 2H), 4.47 (t, J = 6.8Hz, 2H), 4.29 (t, J = 6.3 Hz, 2H), 4.04 (s, 3H), 3.43 (s, 2H), 3.22 (t, J = 6.9 Hz, 2H), 2.43–2.17 (m, 4H), 2.14–2.05 (m, 2H), 1.87–1.76 (m, 2H), 1.59–1.28 (m, 4H), 0.81 (t, J = 7.2 Hz, 6H); LC/MS (ESI) m/z: $[M-Br]^+$ 558.2; HRMS m/z $[M-Br]^+$ Calcd for $C_{32}H_{39}N_5O_4$ 558.3080, Found 558.3072.

4.4.11. 9-*O*-{3-{4-[(*N*,*N*-Di-isopropyl-amino)methyl]-1*H*-1,2,3-triazol-1-yl}propyl}berberine bromide (16c)

Intermediate **4c** was treated with $CuSO_4$, sodium ascorbate and *N*,*N*-diisopropylprop-2-yn-1-amine (**10**) according to general procedure to give the target product **16c** as yellow solid. Yield 40.5%; mp 182.3–183.1; ^{1}H NMR (400 MHz,) δ 9.83 (s, 1H), 8.93 (s, 1H), 8.19 (d, J = 9.2 Hz, 1H), 8.00 (d, J = 9.1 Hz, 1H), 7.91 (s, 1H), 7.79 (s, 1H), 7.10 (s, 1H), 6.17 (s, 2H), 4.97 (t, J = 6.0 Hz, 2H), 4.65 (t, J = 6.8 Hz, 2H), 4.26 (t, J = 6.0 Hz, 2H), 4.03 (s, 3H), 3.64 (s, 2H), 3.23 (t, J = 6.7 Hz, 2H), 3.02–2.92 (m, 2H), 2.45–2.40 (m, 2H), 0.95 (d, J = 6.6 Hz, 12H); HRMS m/z $[M-Br]^+$ Calcd for $C_{31}H_{37}N_5O_4$ 544.2924, Found 544.2929.

4.4.12. 9-*O*-{3-{4-[(*N*,*N*-Di-isopropyl-amino)methyl]-1*H*-1,2,3-triazol-1-yl}butyl}berberine bromide (16d)

Intermediate **4d** was treated with $CuSO_4$, sodium ascorbate and *N*,*N*-diisopropylprop-2-yn-1-amine (**10**) according to general procedure to give the target product **16d** as yellow solid. Yield 37.3%; mp 187.8–188.9; ^{1}H NMR (400 MHz,) δ 9.74 (s, 1H), 8.92 (s, 1H), 8.19 (d, J = 9.2 Hz, 1H), 7.99 (d, J = 9.1 Hz, 1H), 7.86 (s, 1H), 7.79 (s, 1H), 7.09 (s, 1H), 6.17 (s, 2H), 4.95 (t, J = 6.2 Hz, 2H), 4.44 (t, J = 6.9 Hz, 2H), 4.28 (t, J = 6.4 Hz, 2H), 4.04 (s, 3H), 3.62 (s, 2H), 3.22 (t, J = 6.1 Hz, 2H), 3.00–2.93 (m, 2H), 2.11–2.04 (m, 2H), 1.84–1.77 (m, 2H), 0.95 (d, J = 6.6 Hz, 12H); HRMS m/z $[M-Br]^+$ Calcd for $C_{32}H_{39}N_5O_4$ 558.3080, Found 558.3082.

4.4.13. 9-*O*-{3-[4-(Benzyl)-1*H*-1,2,3-triazol-1-yl]proyl}berberine bromide (17c)

Intermediate **4c** was treated with $CuSO_4$, sodium ascorbate and phenyl acetylene according to general procedure to give the target product **17c** as yellow semisolid. Yield 38.6%; ^{1}H NMR (400 MHz,) δ 9.85 (s, 1H), 8.92 (s, 1H), 8.67 (s, 1H), 8.19 (d, J = 9.2 Hz, 1H), 7.99 (d, J = 9.1 Hz, 1H), 7.83 (d, J = 7.1 Hz, 2H), 7.79 (s, 1H), 7.44 (dd, J = 7.1, 7.5 Hz, 2H), 7.33 (t, J = 7.4 Hz, 1H), 7.10 (s, 1H), 6.18 (s, 2H), 4.97 (t, J = 6.1 Hz, 2H), 4.75 (t, J = 6.8 Hz, 2H), 4.33 (t, J = 6.0 Hz, 2H), 4.02 (s, 3H), 3.23 (t, J = 6.9 Hz, 2H), 2.58–2.54 (m, 2H); LC/MS (ESI) m/z: $[M-Br]^+$ 507.2; HRMS m/z $[M-Br]^+$ Calcd for $C_{30}H_{27}N_4O_4$ 507.2032, Found 507.2035.

4.4.14. 9-*O*-{3-[4-(Benzyl)-1*H*-1,2,3-triazol-1-yl]butyl}berberine bromide (17d)

Intermediate **4d** was treated with $CuSO_4$, sodium ascorbate and phenyl acetylene according to general procedure to give the target product **17d** as yellow semisolid. Yield 37.9%; ^{1}H NMR (400 MHz,) δ 9.75 (s, 1H), 8.90 (s, 1H), 8.62 (s, 1H), 8.18 (d, J = 9.2 Hz, 1H), 7.98 (d, J = 9.1 Hz, 1H), 7.82 (d, J = 7.1 Hz, 2H), 7.78 (s, 1H), 7.44 (dd, J = 7.2, 7.4 Hz, 2H), 7.33 (t, J = 7.4 Hz, 1H), 7.09 (s, 1H), 6.17 (s, 2H), 4.93 (t, J = 5.9 Hz, 2H), 4.53 (t, J = 6.8 Hz, 2H), 4.32 (t, J = 6.3 Hz, 2H), 4.04 (s, 3H), 3.20 (t, J = 6.8 Hz, 2H), 2.18–2.11 (m, 2H), 1.90–1.84 (m, 2H); LC/MS (ESI) m/z: $[M-Br]^+$ 521.3; HRMS m/z $[M-Br]^+$ Calcd for $C_{31}H_{29}N_4O_4$ 521.2243, Found 521.2250.

4.4.15. 9-*O*-{3-[4-(Butyl)-1*H*-1,2,3-triazol-1-yl]propyl}berberine bromide (18c)

Intermediate **4c** was treated with $CuSO_4$, sodium ascorbate and 1-hexyne according to general procedure to give the target product **18c** as yellow semisolid. Yield 39.7%; ^{1}H NMR (400 MHz,) δ 9.84 (s, 1H), 8.92 (s, 1H), 8.17 (d, J = 9.1 Hz, 1H), 8.00 (d, J = 9.1 Hz, 1H), 7.94 (s, 1H), 7.77 (s, 1H), 7.08 (s, 1H), 6.16 (s, 2H), 4.98 (t, J = 5.8 Hz, 2H), 4.64 (t, J = 6.6 Hz, 2H), 4.27 (t, J = 5.7 Hz, 2H), 4.02 (s, 3H), 3.23 (t, J = 6.8 Hz, 2H), 2.60 (t, J = 7.5 Hz, 2H), 2.45–2.37 (m, 2H), 1.62–1.49 (m, 2H), 1.37–1.24 (m, 2H), 0.86 (t, J = 7.3 Hz, 3H); LC/MS (ESI) m/z: $[M-Br]^+$ 487.2; HRMS m/z $[M-Br]^+$ Calcd for $C_{28}H_{31}N_4O_4$ 487.2304, Found 487.2308.

4.4.16. 9-*O*-{3-[4-(Butyl)-1*H*-1,2,3-triazol-1-yl]butyl}berberine bromide (18d)

Intermediate **4d** was treated with $CuSO_4$, sodium ascorbate and 1-hexyne according to general procedure to give the target product **18d** as yellow ssemiolid. Yield 38.1%; ^{1}H NMR (400 MHz,) δ 9.77 (s, 1H), 8.95 (s, 1H), 8.18 (d, J = 9.0 Hz, 1H), 7.99 (d, J = 9.2 Hz, 1H), 7.90 (s, 1H), 7.79 (s, 1H), 7.09 (s, 1H), 6.17 (s, 2H), 4.97 (t, J = 6.3 Hz, 2H), 4.43 (t, J = 6.8 Hz, 2H), 4.29 (t, J = 6.1 Hz, 2H), 4.04 (s, 3H), 3.22 (t, J = 6.7 Hz, 2H), 2.58 (t, J = 7.6 Hz, 2H), 2.13–2.02 (m, 2H), 1.88–1.76 (m, 2H), 1.59–1.48 (m, 2H), 1.37–1.24 (m, 2H), 0.88 (t, J = 7.3 Hz, 3H); LC/MS (ESI) m/z: $[M-Br]^+$ 501.3; HRMS m/z $[M-Br]^+$ Calcd for $C_{29}H_{33}N_4O_4$ 501.2532, Found 501.2529.

4.5. Biological activity

4.5.1. In vitro inhibition studies on AChE and BuChE

Acetylcholinesterase (AChE, E.C. 3.1.1.7, from electric eel), butylcholinesterase (BuChE, E.C. 3.1.1.8, from equine serum), 5,5′-dithiobis-(2-nitrobenzoic acid) (Ellman′s reagent, DTNB), acetylthiocholine chloride (ATC) and butylthiocholine chloride (BTC) were purchased from Sigma Aldrich. Berberine derivatives were dissolved in DMSO and then diluted in 0.1 M KH_2PO_4/K_2HPO_4 buffer (pH 8.0) to provide a final concentration range.

4.5.2. In vitro AChE assay

All the assays were carried out under 0.1 M KH_2PO_4/K_2HPO_4 buffer, pH 8.0, using a Shimadzu UV-2450 Spectrophotometer. AChE and BuChE solutions were prepared to give 2.0 units/mL in 2 mL aliquots. The assay medium (1 mL) consisted of phosphate buffer (pH 8.0), 50 μl of 0.01 M DTNB, 10 μl of enzyme, and 50 μl of 0.01 M substrate (ACh chloride solution). Test compounds were added to the assay solution and preincubated at 37 °C with the enzyme for 15 min followed by the addition of substrate. The activity was determined by measuring the increase in absorbance at 412 nm at 1 min intervals at 37 °C. Calculations were performed according to the method of the equation in Ellman et al.[21] Each concentration was assayed in triplicate.

In vitro BuChE assay was similar with the method described above.

4.6. Determination of the inhibitory effect on the self-mediated Aβ(1-42) aggregation

HFIP pretreated $A\beta_{1-42}$ samples (AnaSpec) were resolubilized with a 50 mM phosphate buffer (pH 7.4) in order to have a stable stock solution ([Aβ] = 200 μM).[22] The peptide was incubated in 50 mM phosphate buffer (pH 7.4) at 37 °C for 48 h (final Aβ concentration 50 μM) with and without the tested compound at 20 μM. After incubation, the samples were diluted to a final volume of 200 uL with 50 mM glycine–NaOH buffer (pH 8.0) containing thioflavin T. Then, a 300-seconds-time scan of fluorescence intensity was performed (λ_{exc} = 450 nm; λ_{em} = 485 nm), and values at plateau were averaged after subtracting the background fluorescence of thioflavin T solution.

4.7. Kinetic characterization of AChE inhibition

Kinetic characterization of AChE was performed using a reported method.[23] Test compound was added into the assay solution and pre-incubated with the enzyme at 37 °C for 15 min, followed by the addition of substrate. Kinetic characterization of the hydrolysis of ATC catalyzed by AChE was carried out spectrometrically at 412 nm. A parallel control was made with the assay solution of no inhibitor for each times. The plots were assessed by a weighted least squareanalysis that assumed the variance of V to be a constant percentage of V for the entire data set. Slopes of these reciprocal plots were then plotted against the concentration of the inhibitors in a weighted analysis and K_i was determined as the ratio of the replot intercept to the replot slope.

4.8. Molecular modeling

The simulation system was built based on the X-ray crystal structure of the bis(7)tacrine-AChE complex which was obtained from the Protein Data Bank (PDB entry 2CMF). The original ligand was removed while water molecules present in the PDB file were maintained in their position. 3D structures of the 9-substituted berberine derivatives were generated and optimized by DISCOVERY studio 2.1 package (Accelrys Inc., San Diego, CA). The CDOCKER

program in DISCOVERY STUDIO 2.1 software was used to perform docking simulations, which allows full flexibility of the ligand.

Acknowledgments

We thank the Natural Science Foundation of China (20972198) and the Ministry of Science and Technology of China (No. 2009ZX09501-017) for financial support of this study.

References and notes

1. Bemis, G. W.; Murcko, M. A. . *J. Med. Chem.* **1996**, *39*, 2887.
2. Kolb, H. C.; Finn, M. G.; Sharpless, K. B. *Angew. Chem., Int. Ed.* **2001**, *40*, 2004.
3. Zhang, H.; Ryono, D. E.; Devasthale, P. *Bioorg. Med. Chem. Lett.* **2009**, *19*, 1451.
4. Calvo-Flores, F. G.; Isac-Garcia, J.; Hernandez-Mateo, F. *Org. Lett.* **2000**, *2*, 2499.
5. Perez-Balderas, F.; Ortega-Munoz, M.; Morales-Sanfrutos, J. *Org. Lett.* **2003**, *5*, 1951.
6. Lewis, W. G.; Green, L. G.; Grynszpan, R. *Angew. Chem., Int. Ed.* **2002**, *41*, 1053.
7. Whiting, M.; Muldoon, J.; Lin, Y. C. *Angew. Chem., Int. Ed.* **2006**, *45*, 1435.
8. Alvarez, R.; Velazquez, S.; San-Felix, A.; Balzarini, J.; Camarasa, M. J. *J. Med. Chem.* **1994**, *37*, 4185.
9. Genin, M. J.; Allwine, D. A.; Anderson, D. J. *J. Med. Chem.* **2000**, *43*, 953.
10. Natarajan, A.; Du, W.; Xiong, C. Y.; DeNardo, G. L.; DeNardo, S. J.; Gervay-Hague, J. *Chem. Commun.* **2007**, *7*, 695.
11. Bourne, Y.; Kolb, H. C.; Radic, Z.; Sharpless, K. B.; Taylor, P.; Marchot, P. *Proc. Natl. Acad. Sci. U.S.A.* **2004**, *101*, 1449.
12. Krasinski, A.; Radic, Z.; Manetsch, R.; Raushel, J.; Taylor, P.; Sharpless, K. B.; Kolb, H. C. *J. Am. Chem.* **2005**, *127*, 6686.
13. Recanatini, M.; Valenti, P. *Curr. Pharm. Des.* **2004**, *10*, 3157.
14. Isabel, F. B.; Concepcion, P.; Nuria, E.; Juan, A. P.; Gema, C. G.; Paola, U.; Esther, G. P.; Manuela, G. L.; Mercedes, V.; Antonio, G. G.; Ana, M.; Isabel, R. F. *Chem. Med. Chem.* **2009**, *4*, 828.
15. Guillou, C.; Mary, A.; Renko, D. Z.; Gras, E.; Thal, C. *Bioorg. Med. Chem. Lett.* **2000**, *10*, 637.
16. Xie, Q.; Wang, H.; Xia, Z.; Lu, M.; Zhang, W.; Wang, X.; Fu, W.; Tang, Y.; Sheng, W.; Li, W.; Zhou, W.; Zhu, X.; Qiu, Z.; Chen, H. *J. Med. Chem.* **2008**, *51*, 2027.
17. Huang, L.; Shi, A. D.; He, F.; Li, X. S. *Bioorg. Med. Chem.* **2010**, *18*, 1244.
18. Iwasa, K.; Kamigauchi, M.; Ueki, M.; Taniguchi, M. *Eur. J. Med. Chem.* **1996**, *31*, 469.
19. Zhang, W. J.; Ou, T. M.; Lu, Y. J.; Huang, Y. Y.; Wu, W. B.; Huang, Z. S.; Zhou, J. L.; Wong, K. Y.; Gu, L. Q. *Bioorg. Med. Chem.* **2007**, *15*, 5493.
20. Tsou, H. R.; Mamuya, N.; Johnson, B. D. *J. Med. Chem.* **2001**, *17*, 2719.
21. Ellman, G. L.; Courtney, K. D.; Andres, B. Jr.; Featherstone, R. M. *Biochem. Pharmacol.* **1961**, *7*, 88.
22. Michela, R.; Elena, S.; Manuela, B. *J. Med. Chem.* **2008**, *51*, 4381.
23. Maria, L. B.; Vincenza, A.; Manuela, B.; Rita, B.; Carlo, M. J. *Med. Chem.* **2005**, *48*, 24.